Hydrometallurgy 157 (2015) 356–362

Contents lists available at ScienceDirect

Hydrometallurgy

journal homepage: www.elsevier.com/locate/hydromet

Recovery of yttrium and lanthanides from sulfate solutions with high concentration of iron and low rare earth content

Denis Beltrami *, Gauthier J.-P. Deblonde, Sarah Bélair, Valérie Weigel

ERAMET Research, Hydrometallurgy Department, 1 avenue Albert Einstein, F-78193 Trappes, France

ARTICLE INFO

Article history:
Received 24 March 2015
Received in revised form 19 June 2015
Accepted 26 July 2015
Available online 1 August 2015

Keywords:
Rare earths
Precipitation
Phosphate rare earths
Low REE concentrations

ABSTRACT

To overcome the low recovery, generally obtained for the heavy and middle rare earth elements (HREE and MREE) by sodium double sulfate precipitation, the recovery of the MREE and HREE as phosphate salts was investigated. High recovery yields (≥95%) were obtained even for sulfate solutions containing low concentrations of REE and a high concentration of iron(II). The influence of many industry-relevant parameters (temperature, pH, stoichiometric excess of phosphate, aluminum contamination, residence time) is discussed in order to optimize the REE recovery and to minimize the precipitation of iron. The developed process was also validated in continuous operation at a pilot scale. Finally, the REE phosphate concentrate could be converted into REE hydroxides which allows its dissolution into diluted HCl. Taking into account the phosphate precipitation, the conversion into hydroxides and the dissolution in $HCl_{(aq)}$, high recovery yields were obtained for Y, Gd and La (68%, 77% and 86% respectively). The results show that it is possible to economically obtain purified REE solutions starting from industrial solutions which are usually discarded.

1. Introduction

Rare earth elements (REEs) namely, scandium, yttrium and lanthanides, play a critical role on the global economy due to the numerous applications where those elements are used. Rare earth-based materials are used in electronic industry, steel industry, household batteries, fluorescent lamps, permanent magnets, and lasers for surgical and nuclear technologies (Alonso et al., 2012; Gupta and Krishnamurthy, 2005). The global consumption of REE exceeded 100,000 t in 2011 and is expected to double by 2020 with an annual growth rate of 4 to 9% (Alonso et al., 2012; Tan et al., 2014). Among the rare earth elements, some are more critical for industrial applications and their supply might be threatened in the next decades. In particular, Nd, Eu, Tb, Dy and Y are expected to become highly strategic metals in the future (Golve et al., 2014; U.S. Department of Energy, 2011). For instance, the global demand for Nd and Dy is projected to grow by 700% and 2600% in the next 25 years (Alonso et al., 2012).

Even if an intensive effort is being made worldwide to recycle REE from waste electronic equipments, magnets or waste fluorescent lamps (Binnemans et al., 2013; Tan et al., 2014; Yang et al., 2014), the REEs are still mainly recovered from natural minerals like monazite [$(Ce, La, Y)PO_4$], xenotime (YPO_4) and bastnasite [$(La, Ce)CO_3F$].

Since the early 2000s, the recovery of REE from a Gabonese ore, called Maboumine, has been studied by ERAMET. The Maboumine deposit not only accounts for one of the main sources of Nb for the future but also contains other valuable elements as given in Table 1 (Chakhmouradian et al., 2015; Mitchell, 2015). In the hydrometallurgic process developed by ERAMET, almost 90% of the light REEs (LREE: La, Ce, Pr and Nd) and 50% of the medium REEs (MREE: Sm, Eu, Gd, Tb and Dy) are precipitated as double sulfate salts (Belair and Weigel, 2014). Nonetheless, only 10% of the heavy REEs (HREE: Ho, Er, Tm, Yb and Lu) are recovered by this process and, as a result, nearly 400 mg L^{-1} REEs remain in solution after the double sulfate salt precipitation.

In this paper, a brief review of REE recovery from leach liquors produced by acid or alkaline decomposition is presented. Experimental work was conducted on a process for the recovery of yttrium and lanthanides from sulfate solutions containing low concentrations of REE, a low content of aluminum and a high excess of iron as previously reported in a patent (Vincec, 2014). The influence of many industry-relevant parameters is discussed like the residence time, the temperature of the media, the aluminum contamination, the pH of precipitation and the stoichiometric excess of the reagent. The effect of these parameters on the quality of the precipitate is studied and pilot-scale tests on industrial solutions were performed in order to demonstrate the validity of the proposed process. Finally, purification steps of the REE concentrate, i.e. caustic soda conversion into REE hydroxides and dissolution into chloride media, were investigated.

2. Process for REE recovery

Monazites generally contain 35–71% of rare earth oxides (REO) whereas xenotime and bastnasite commonly contain 52–54% and 70–

* Corresponding author.
E-mail address: denis.beltrami@erametgroup.com (D. Beltrami).

http://dx.doi.org/10.1016/j.hydromet.2015.07.015
0304-386X/

Table 1
Typical composition of the Maboumine Ore.

Element	Fe	Al	P	REE	Nb	Ta	U
% (w/w)	35	6.1	2.7	1.4	1.2	0.03	0.03

74% of REO, respectively (Jordens et al., 2013; Kanazawa and Kamitani, 2006). After ore beneficiation by physical treatments (gravity separation, desliming, magnetic separation, electrostatic separation or froth flotation), the recovery of REE from natural ores is performed by hydrometallurgical processes. Conventional hydrometallurgical processes for the recovery of REE can be classified into two main classes:

(i) acid decomposition of the natural minerals and dissolution of the REE in acidic media (generally $H_2SO_{4(aq)}$). Then the valuable elements are precipitated as oxalates $(REE)_2(C_2O_4)_3$, $nH_2O_{(s)}$ or double sulfate salts $NaREE(SO_4)_2$, $nH_2O_{(s)}$ as described in Eqs. (1) and (2) (Abreu and Morais, 2010; Anvia et al., 2015; Kul et al., 2008). Those precipitates are then purified to obtain a REE concentrate or a REE commercial salt (chloride, carbonate, fluoride etc.). It should be noted that solvent extraction can also be implemented directly after the ore leaching to produce a REE concentrate or to directly separate the REE (Xie et al., 2014).

$$2\,REE^{3+} + 3\,C_2O_4^{2-} + n\,H_2O = (REE)_2(C_2O_4)_3, nH_2O_{(s)} \quad (1)$$

$$REE^{3+} + 2\,SO_4^{2-} + Na^{+} + n\,H_2O = NaREE(SO_4)_2, nH_2O_{(s)} \quad (2)$$

(ii) alkaline decomposition of the natural ores to produce a REE hydroxide concentrate that can then be dissolved selectively in acidic media (generally $HCl_{(aq)}$) as given in Eqs. (3) and (4) (Panda et al., 2014). After precipitation of the remaining impurities, the REE solution can feed a solvent extraction process in order to separate the REE.

$$REEPO_{4(s)} + 3\,NaOH_{(aq)} = REE(OH)_{3(s)} + Na_3PO_{4(aq)} \quad (3)$$

$$REE(OH)_{3(s)} + 3\,HCl_{(aq)} = REECl_{3(s)} + 3\,H_2O \quad (4)$$

For bastnasite ores [(La, Ce)CO_3F], a mixture of the two routes described above can also be used (Bian et al., 2011; Gupta and Krishnamurthy, 2005; Kul et al., 2008). This consists of the carbonate removal by acid treatment followed by the alkaline decomposition of the remaining $REEF_3$, as described below.

$$3REEFCO_{3(s)} + 6\,H^{+} = REEF_{3(s)} + 2\,REE^{3+} + 3H_2O + 3CO_2 \quad (5)$$

$$REEF_{3(s)} + 3\,NaOH_{(aq)} = REE(OH)_{3(s)} + 3NaF_{(aq)} \quad (6)$$

Rare earth elements can also be recovered, as by-products, from the uranium or phosphoric acid productions (Beltrami et al., 2014; Bunus, 2000; Bunus and Dumitrescu, 1992; Bunus et al., 1994). For example, yttrium has occasionally been recovered as a by-product of uranium ores from Ontario. Other mining sites like Olympic Dam, which produces copper, uranium, gold and silver, could also produce REE in the next decades (Esdale et al., 2003). In these particular systems, the concentration of REE is rather low compared to the traditional REE ores and the impurity content is high. Hence, the classical routes of precipitation (i.e. REE oxalate and REE double sulfate salts) would not be economical, especially to recover the middle and heavy rare earth elements.

The REE precipitation by the addition of oxalic acid is effective owing to the strong affinity of the oxalate ion for hard ions like REE^{3+} and due to the low solubility of REE oxalate precipitates. Nonetheless, oxalic acid is an expensive reagent and the release of carbon dioxide during the calcination of $(REE)_2(C_2O_4)_3$,$nH_2O_{(s)}$ could raise environmental concerns. Regarding the REE double sulfate salt precipitation, the quantitative recovery of HREE requires a very high excess of sodium ions. Little detailed information is available on REE double salt precipitation but it seems that the solubility of $NaREE(SO_4)_2$,$nH_2O_{(s)}$ increases with the atomic number of the REE (Lokshin et al., 2005, 2007). To treat these low REE concentration solutions, ion exchange and solvent extraction systems have been extensively studied (Radhika et al., 2010, 2011; Reddy et al., 2009).

3. Experimental

3.1. Materials

Powder XRD spectra were collected using Cu $K_{\alpha 1}$ radiation with a wavelength of 1.54053 Å. Diffraction patterns were obtained using a Panalytical X'Pert Pro diffractometer and identified with the software HighScore (Panalytical).

The concentrations of aluminum (Al), iron (Fe), phosphorus (P), sulfur (S), cerium (Ce), lanthanum (La), neodymium (Nd), gadolinium (Gd), praseodymium (Pr) and yttrium (Y) were determined by ICP–OES using an iCAP 6000 series spectrometer (Thermo Scientific). Other REEs were determined by ICP–MS using an Aurora M90 spectrometer (Bruker). Samples were diluted in 2% (v/v) HNO_3 for analysis. Quantitative analyses were performed at 308.215 nm, 238.204 nm, 177.434 nm, 180.669 nm, 446.021 nm, 333.749 nm, 410.945 nm, 336.224 nm, and 371.029 nm spectral emission lines for Al, Fe, P, S, Ce, La, Nd, Gd and Y respectively. The limit of quantitation of our method was 0.5 mg L^{-1} in the initial sample. Sodium (Na) concentrations were determined by flame absorption spectroscopy using an AA 220 spectrometer (Varian) and 589.6 nm spectral emission line.

The pH measurements were performed with an 827 pH-lab (Metrohm) pH-meter and low alkaline error combined electrode (Unitrode, Metrohm). The pH-meter was calibrated with NIST standards at pH 4.00, 7.00 and 12.00. The electropotential was measured with a Mettler Toledo type 1120 device, the reference electrode was a Ag/AgCl, KCl (3 mol L^{-1}).

3.2. Reagents

Sodium phosphate dodecahydrate (Sigma Aldrich, 96%), aluminum sulfate octadecahydrate (VWR, 97%), phosphoric acid solution (Sigma Aldrich, 85%), sulfuric acid solution (VWR, 96%), sodium hydroxide solution (VWR, 50%), nitric acid solution (VWR, 65%) and calcium hydroxide (Sigma Aldrich, 96%) were used as received. The REE solution used in this study was provided by ERAMET Research (France) and comes from the Maboumine hydrometallurgical process (Agin et al., 2012; Belair and Weigel, 2014; Donati et al., 2014). The major part of the REE, initially present in the solution, was precipitated by double sulfate salt precipitation as described elsewhere (Vincec, 2014). Then an aluminum bleed was performed with a 20% (w/w) $Ca(OH)_2$ slurry in order to precipitate the major part of the aluminum ($AlOHSO_{4(s)}$, $AlPO_{4(s)}$ and $Al(OH)_{3(s)}$). The elimination of aluminum avoids the high consumption of phosphate during the precipitation of the REE (Vincec, 2014). During the aluminum bleed, the concentrations of aluminum and REE varied from 12.50 g L^{-1} and 0.40 g L^{-1} down to 0.03 g L^{-1} and 0.23 g L^{-1}, respectively (Table 2). A part of the REE present in solution is lost by co-precipitation with gypsum. This step is not described in detail in this paper.

The filtrate is used as REE stock solution and its composition is given in Table 2. The sodium concentration was found to be 5.0 g L^{-1} and the pH was 4.3. The potential of the REE stock solution was 150 ± 20 mV (vs Ag/AgCl), meaning that iron was present as Fe(II).

Table 2
Elemental analysis of the REE stock solution used for precipitation tests.

Element	Y	La	Ce	Pr	Nd	Sm	Eu	Gd	Tb	Dy
mg L^{-1}	61	18	73	4	14	13	<1	19	7	11
Element	Ho	Er	Tm	Yb	Lu	∑REE	Fe	Al	P	SO_4
mg L^{-1}	<1	<1	<1	<1	5	230	32,300	30*	30	75,000

* Varied from 30 to 1000 mg L^{-1} (see text).

3.3. Experimental procedure

Precipitation experiments were carried out by adding a mixture of $Na_3PO_{4(aq)}/H_3PO_{4(aq)}$ solution (0.5 mol L^{-1} $H_xPO_4^{x-3}$, x = 1–3) at a given pH to the REE stock solution under stirring at 500 rpm. A 1 L glass reactor was used for precipitation experiments and a probe was set inside the reactor to measure and maintain the temperature at the desired value throughout the experiments. After precipitation, the suspension was centrifuged at 5000 rpm for 15 min. The solid phase was recovered, washed 2 times with 10 mL of water and dried at 60 °C for 24 h. The mass of solid phase obtained was comprised between 0.5 and 12 g. The filtrate was immediately diluted by 2 with 10% (w/w) nitric acid to avoid any precipitation before elemental analysis.

For precipitation experiments performed at different pH values, micro-quantities of 1.5 mol L^{-1} NaOH or 96% (w/w) H_2SO_4 were added in both stock solutions (REE and sodium phosphate solutions) before precipitation to reach the desired pH. Due to the protons released by $H_xPO_4^{x-3}$ ($1 \le x \le 3$) ions during the precipitation of $(REE)PO_{4(s)}$, the pH was controlled during the precipitation by further addition of micro-quantities of 1.5 mol L^{-1} NaOH.

To study the influence of aluminum on the REE precipitation, the required amount of aluminum sulfate octadecahydrate was dissolved in the REE stock solution so that the aluminum concentration varied from 30 to 1000 mg L^{-1}. The volume variation due to the aluminum sulfate octadecahydrate dissolution was found negligible.

The stoichiometric quantity (SQ) mentioned in this work is defined as follows:

$$SQ = \frac{\sum_x H_xPO_4^{x-3} \text{ added (mol)}}{\sum \text{REE initial (mol)}}.$$

The yields of precipitation were calculated from the elemental analysis of the solution before and after precipitation.

4. Results and discussion

The present study investigated the precipitation of yttrium and lanthanides from low concentration sulfate solutions by the addition of sodium phosphate solution. Due to the strong affinity of $Y^{3+}{}_{(aq)}$ and $Ln^{3+}{}_{(aq)}$ ions for $PO_4^{3-}{}_{(aq)}$ compared to $SO_4^{2-}{}_{(aq)}$ (Firsching and Brune, 1991; Kim and Osseo-Asare, 2012) the addition of $Na_3PO_{4(aq)}$ to a sulfate solution of yttrium and lanthanides was expected to trigger the precipitation of REE phosphate (Eq. (7)) even at low concentration of REE.

$$\mathbf{REE(SO_4)_n^{3-2n}_{(aq)} + PO_4^{3-} = REEPO_{4(s)} + n\,SO_4^{2-}} \quad (7)$$

4.1. Factors affecting precipitation efficiency

4.1.1. Effect of temperature and phosphate quantity

The precipitation of REE was investigated at different temperatures between 40 °C and 100 °C (Table 3). High precipitation yields were obtained (≥84%) even with a low excess of sodium phosphate (SQ = 15 mol/mol).

Table 3
Influence of the temperature on the recovery of REE for a fixed quantity of phosphates added. Residence time: 1 h, n_{PO4}/n_{REE} = 15 mol/mol, $[Al]_{initial}$ = 30 mg L^{-1}, $pH_{initial}$ = 4.3.

	Precipitation (%)							
T (°C)	Ce	La	Nd	Gd	Dy	Sm	Y	Fe
40	97.1	89.4	88.6	90.5	83.6	87.7	97.3	3.0
70	99.1	≥97.0	≥96.2	96.6	≥95.2	≥95.9	98.9	3.1
90	≥99.2	≥97.0	≥96.2	≥97.2	≥95.2	≥95.9	≥99.1	3.3
	Final concentration (mg L^{-1})							
T (°C)	Ce	La	Nd	Gd	Dy	Sm	Y	Fe
40	2.0	1.8	1.5	1.7	1.7	1.5	2.5	29,600
70	0.6	0.5[a]	0.5[a]	0.6	0.5[a]	0.5[a]	0.6	28,600
90	0.5[a]	0.5[a]	0.5[a]	0.5[a]	0.5[a]	0.5[a]	0.5[a]	27,700

[a] Limit of quantitation.

It should be highlighted that the sodium concentration resulting from the addition of $Na_3PO_{4(aq)}$ is not enough to obtain such yields by precipitation of the REE double sulfate salts. The final concentration of sodium in the filtrates was 0.31 mol L^{-1} compared to 0.22 mol L^{-1} in the REE feed solution. Similar precipitation tests using $Na_2SO_{4(aq)}$ with the same final concentration of Na^+ resulted in precipitation yields lower than 2% (data not shown). This was confirmed by analysis and characterization of the precipitate (see part 4.2).

For all lanthanides, the precipitation yield increases slightly from 40 °C to 70 °C but the yields obtained at 90 °C and at 70 °C are identical within the experimental uncertainty. A similar effect was observed by Wang et al. (2010) when leaching REE contained in phosphate rocks with sulfuric acid. The solubility of yttrium phosphate and several lanthanide phosphates was also studied by Firsching and Brune (1991) on synthetic samples. The lanthanide phosphates were found to be weakly soluble with solubility limits ranging from $2.1 * 10^{-5}$ mol L^{-1} for terbium to $4.0 * 10^{-4}$ mol L^{-1} for praseodymium at 25 °C and at pH 1.1. No noticeable trend was observed along the lanthanide series and the reported pKs values are in the range of 25.1 for Tb to 26.2 for Pr at 25 °C, where pKs = −log Ks and Ks is the solubility product of the phosphate salt. It was also reported that the pKs values of the $LnPO_{4(s)}$ increase very slightly with the temperature, in accordance with the precipitation yields observed in this work.

To improve the cost-effectiveness of the developed process, the quantity of phosphate vs. REE was studied at constant pH and temperature (Fig. 1). As expected, La, Ce and Nd have a similar behavior. For the sake of clarity, only the analyses for Ce, Gd and Y are given in the next parts of this paper. As expected, the recovery of all the REE is improved when the ratio PO_4/REE increases due to the displacement of Eq. (7) to

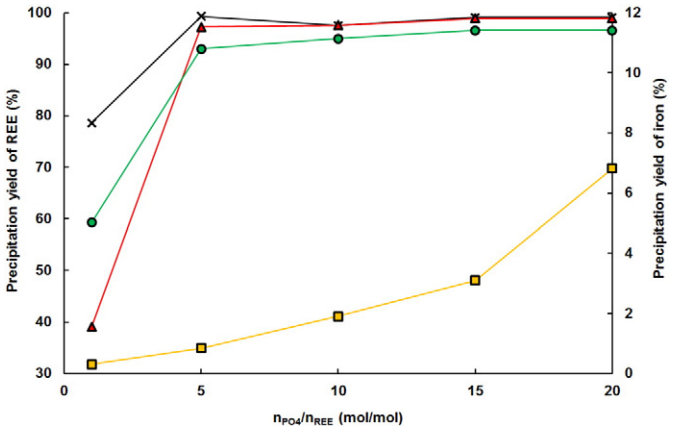

Fig. 1. Influence of the phosphate quantity on the REE recovery (×: Ce, ○: Gd and Δ: Y) and Fe (□). T = 70 °C, residence time = 1 h, pH = 4.0, $[Al]_{initial}$ = 30 mg L^{-1}.

the right. However, higher stoichiometric excess of phosphate ions triggers the precipitation of iron (Eq. (8)).

$$3Fe^{2+} + 2PO_4^{3-} + xH_2O = Fe_3(PO_4)_2.xH_2O_{(s)} \quad (8)$$

The precipitation yield of iron phosphate is rather low compared to the REE phosphates (Fig. 1) but due to the large excess of iron in the initial solution (Table 2), the precipitation of iron has to be kept as low as possible in order to maintain the quality of the REE precipitate. Interestingly, the phosphorus concentration in the filtrates after precipitation was rather low (<30 mg L^{-1}) confirming that the excess of phosphate ions reacts with iron in solution.

4.1.2. Effect of residence time

The precipitation of iron under the conditions given in Fig. 1 was surprising, knowing that iron was present in the form of Fe(II) in the REE stock solution. Then, the influence of the residence time on the precipitation of REE and iron was investigated at constant temperature. No improvement of the REE precipitation yields was observed between 1 h and 6 h meaning that yttrium and the lanthanides are precipitated in less than 60 min. Nonetheless, the precipitation of iron is favored by a long residence time (Fig. 2). This can be explained by the slow oxidation of Fe(II) by ambient oxygen and precipitation of $FePO_{4(s)}$ or $Fe(OH)_{3(s)}$ as depicted below.

$$2\mathbf{Fe}^{2+} + \frac{1}{2}\mathbf{O}_2 + 2\mathbf{H}^+ = 2\mathbf{Fe}^{3+} + \mathbf{H_2O} \quad (9)$$

$$\mathbf{Fe}^{3+} + 3\mathbf{H_2O} = \mathbf{Fe(OH)}_{3(s)} + 3\mathbf{H}^+ \quad (10)$$

$$Fe^{3+} + PO_4^{3-} = FePO_{4(s)} \quad (11)$$

Hence, a short residence combined with a low excess of phosphate ions reduces the precipitation of iron and, therefore, enhances the quality of the REE precipitate without impacting the recovery of the valuable elements.

4.1.3. Effect of aluminum concentration

Another poisoning element that is often present in REE hydrometallurgical processes is aluminum. Compared to ferric ions, which can be easily reduced into ferrous ions, aluminum ion poses major difficulties due to its similarity with REE(III) ions.

The aluminum concentration was varied from 30 mg L^{-1} to 1000 mg L^{-1} in the REE industrial stock solution. This corresponds to a ratio Al/REE varying from 1.8 to 18.5 mol/mol. The results from phosphate precipitation tests are given in Fig. 3. The increase of the aluminum content has a significant effect on the precipitation yield of the $REEPO_{4(s)}$. Due to the hardness of Al^{3+} ion compared to the REE^{3+} ions, the precipitation of $AlPO_{4(s)}$ competes with the precipitation of $REEPO_{4(s)}$ which is in accordance with the reported pKs values for $AlPO_{4(s)}$ and $REEPO_{4(s)}$ (Table 4). The precipitation yields of the REE thus drop to less than 30% with an initial aluminum concentration of 1000 mg L^{-1}, whereas the precipitation yield of aluminum reaches 75%. This confirms that the economical recovery of the REE by phosphate precipitation could not be achieved in the presence of a high excess of aluminum except if an aluminum-scrubbing step is added to the process as described by Vincec (2014).

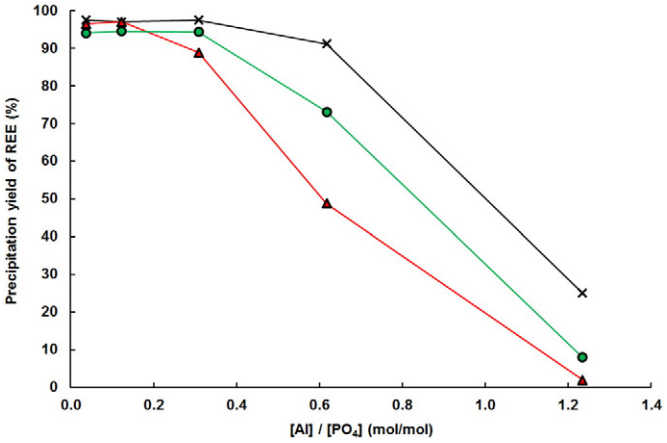

Fig. 3. Influence of the aluminum concentration in feed solution on the REE recovery (×: Ce, ○: Gd and Δ: Y) for a fixed quantity of phosphates added. T = 70 °C, n_{PO4}/n_{REE} = 15 mol/mol, $pH_{initial}$ = 4.3.

4.1.4. Effect of pH

Another relevant parameter that has to be studied while developing hydrometallurgical processes is the solution pH. Concerning the system investigated in this work, several proton-equilibria take place. Indeed, the REE^{3+}, Al^{3+} and Fe^{3+} ions can be easily hydrolyzed and the phosphate ion, used to precipitate the REE, can be simply, doubly or triply protonated. Therefore, the pH of precipitation was expected to play a major role on the precipitation of $REEPO_{4(s)}$.

Fig. 4 shows the speciation diagram for La(III) at 25 °C under the conditions used in this study. The speciation diagram of lanthanum could be calculated because it is the only REE for which the formation constants of the sulfate and hydroxide complexes were published as well as the solubility products of $La(OH)_{3(s,\ am)}$, $LaPO_{4(s)}$ and $LaNa(SO_4)_2,H_2O$ (Lokshin et al., 2005; Smith et al., 2004). Fig. 5 gives the yields of precipitation of the REE and iron. The theoretical diagram and the experimental results are in good agreement (Figs. 4 and 5). As the pH decreases, the yield of precipitation of the $REEPO_{4(s)}$ decreases, falling to 0% at pH 2. This trend is due to the competition between the protonation of the phosphate ions and their precipitation by the REE^{3+} ions. A total

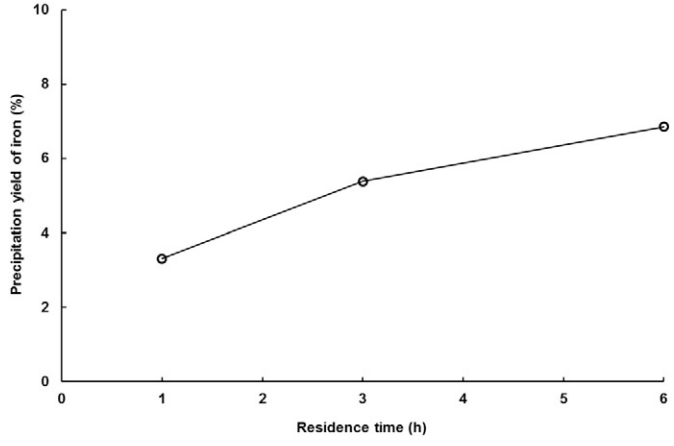

Fig. 2. Influence of residence time on iron precipitation. T = 70 °C, n_{PO4}/n_{REE} = 15 mol/mol, pH = 4.0, $[Al]_{initial}$ = 30 mg L^{-1}.

Table 4
Ionic radius of Al^{3+}, La^{3+}, Ce^{3+} and Gd^{3+} (Shannon, 1976) and pKs values of $AlPO_{4(s)}$, $LaPO_{4(s)}$, $CePO_{4(s)}$ and $GdPO_{4(s)}$ (Smith et al., 2004).

Metal	Ionic radius (pm)	pKs $MPO_{4(s)}$
Al^{3+}	53.5[a]	18.3 (T = 37 °C, I = 0.15 mol L^{-1})
La^{3+}	103[a]	22.43
	116[a]	(T = 25 °C, I = 0.5 mol L^{-1})
Ce^{3+}	101[a]	26.3
	114[b]	(T = 25 °C, I = 0 mol L^{-1})
Gd^{3+}	93.8[a]	25.6
	105[b]	(T = 25 °C, I = 0 mol L^{-1})

[a] For a coordination number of 6.
[b] For a coordination number of 8.

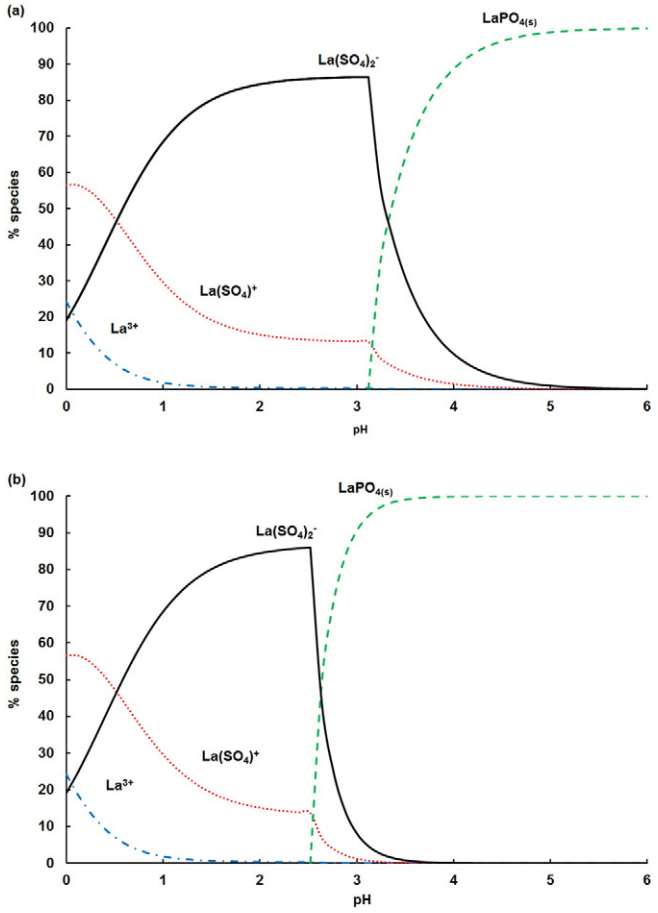

Fig. 4. Speciation diagrams of La(III) at 25 °C. (a): ∑ H_xPO4/REE = 1 mol/mol. (b): ∑ H_xPO4/REE = 15 mol/mol. [La]total = 10^{-4} mol L^{-1}, [Na^+] = 0.22 mol L^{-1} and [SO_4^{2-}] = 0.78 mol L^{-1}. The formation constants used to draw the diagrams are given in Appendix I. Hyss software was used for the drawing of the diagram (Alderighi et al., 1999).

recovery is achieved for pH ≥ 4. In the case of iron, the precipitation yield starts to increase at pH 3 due to the precipitation of $Fe(OH)_3$, $FePO_{4(s)}$ and $Fe_3(PO_4)_2.xH_2O_{(s)}$. Hence, precipitation at pH 4 gives the best compromise between the quantitative REE recovery and iron contamination. Regarding aluminum (30 mg L^{-1} in the feed solution), a quantitative precipitation was observed in the pH range investigated

Table 5
Composition of the REE precipitate obtained during the pilot campaign.

Element	Y	La	Ce	Gd	∑REE	Al	Fe	P	S	Na
% (w/w)	5.8	1.7	7.5	2.0	22.1	1.8	12.5	10.0	1.4	0.2

highlighting the need for the addition of an aluminum-scrubbing step in the process.

4.2. Validation of REE recovery at pilot scale and characterization of REE solid

In order to validate the precipitation process developed at the laboratory scale, the recovery of REE from industrial sulfate solution (Table 2) was tested in a continuous operation at the pilot scale. The process was operated for 10 days at steady-state conditions. For the reason mentioned above, the REE precipitation was performed at pH 4.0 (±0.2), at 70 °C, with a residence time of 1 h and with a stoichiometric excess (n_{PO4}/n_{REE}) of 4 to 5 mol/mol. The flow rate of the REE stock solution was 25 L h^{-1}.

A good REE recovery was obtained during the pilot campaign with an average precipitation yield higher than 95% for all the REEs initially present in the sulfate solution and about 6 kg of REE concentrate was produced. The residual concentrations of the REE after phosphate precipitation were lower than the limit of quantitation (0.5 mg L^{-1}). Regarding iron, the average precipitation yield was 0.35% during the pilot campaign compared to 0.85% obtained in similar conditions at the laboratory scale (Fig. 1). This is due to a better control of the oxidation of iron(II) by the air when larger reaction vessels are used. The average composition of the solid obtained by phosphate precipitation is given in Table 5. Even if the REE concentration in the feed solution was low and the iron concentration was high (Table 2), a REE concentrate was obtained. The ratio Fe/ΣREE was greatly reduced dropping from 140 g/g in the initial solution to 0.6 g/g in the REE precipitate. The presence of sodium in the REE concentrate, however low, indicates that a small amount of REE has precipitated as sodium double sulfate salts. This precipitation was not predicted by the speciation diagram given in Fig. 4, where no $NaLa(SO_4)_2,H_2O_{(s)}$ is formed. This could convey the effect of the temperature on the precipitation of the REE double sulfate salts because the process was operated at 70 °C whereas the speciation diagram is given at 25 °C. Indeed, the decrease of the solubility of the $NaREE(SO_4)_2,nH_2O_{(s)}$ with increasing temperature was reported by Pietrelli et al. (2002).

The XRD analysis of the REE concentrate indicates that the solid is mainly amorphous (Fig. 6). It should be noted that xenotime or

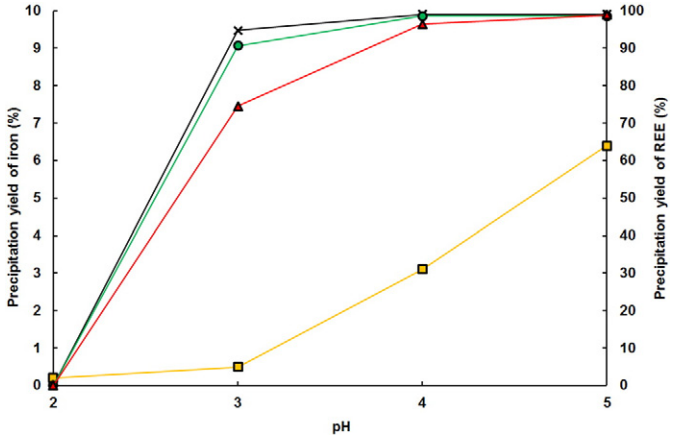

Fig. 5. Influence of the pH of precipitation on the REE (×: Ce, ○: Gd and Δ: Y) and iron (□) recovery. T = 70 °C, residence time = 1 h, n_{PO4}/n_{REE} = 15 mol/mol.

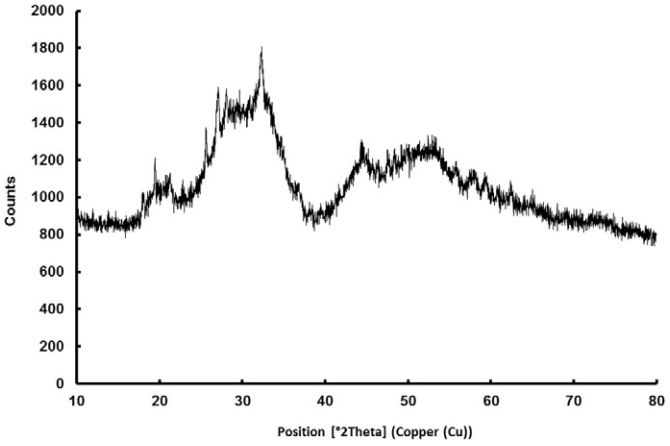

Fig. 6. XRD spectrum of the REE precipitate obtained by phosphate precipitation at pilot scale and dried at 60 °C.

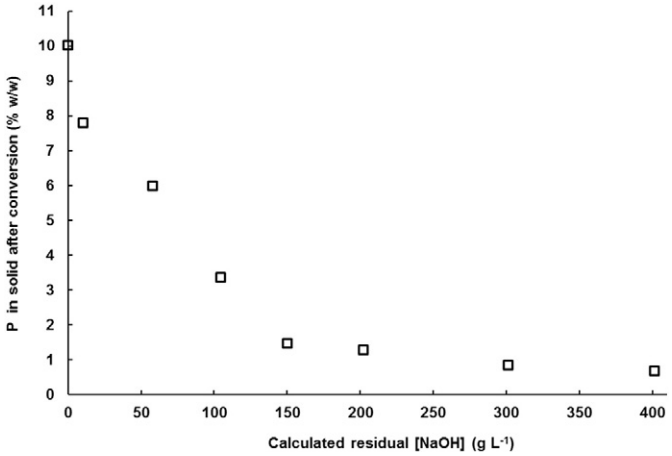

Fig. 7. Residual phosphorous concentration in the REE concentrate after alkaline conversion as a function of the residual NaOH concentration. T = 6 h. Temperature = $NaOH_{(aq)}$ boiling point. The temperature varied from left to right as follows: 100 °C, 100 °C, 100 °C, 101 °C, 102 °C, 106 °C, 112 °C and 118 °C. The residual NaOH concentration was calculated according to the following formula: $[NaOH]_{residual} = M_{NaOH} * (C_{Na} - 3 * C_P - 2 * C_S - C_{Al})$ where M_{NaOH} and C_M refer to the molecular weight and the molar concentration at equilibrium, respectively. This formula considers the presence of $NaAl(OH)_4$, Na_2SO_4 and Na_3PO_4 species in solution. Initial solid to liquid ratio: 100 g of dried solid for 1 L of NaOH solution.

monazite structures were not observed. Likewise, no diffraction peak corresponding to $NaREE(SO_4)_2{,}nH_2O_{(s)}$ was observed.

4.3. Purification of phosphate REE concentrate

As highlighted in Table 5, the REE concentrate obtained by phosphate precipitation contains a significant amount of iron and, as expected, phosphorous. Phosphate has to be removed from the REE precipitate so that the valuable elements can be dissolved in the appropriate media (Eqs. (3) and (4)).

The REE concentrate was treated with $NaOH_{(aq)}$ with the objective of eliminating phosphorous by converting $REEPO_{4(s)}$ into $REE(OH)_{3(s)}$. Batch conversions were performed on the precipitate obtained at the pilot scale. The tests were done at boiling point under atmospheric pressure with various $NaOH_{(aq)}$ concentrations so that the reaction temperature can be increased. In order to follow the conversion of $REEPO_{4(s)}$, the phosphorous content in the solid was measured as a function of the $NaOH_{(aq)}$ concentration at equilibrium.

Fig. 7 shows a clear decrease of the phosphorous content in the REE precipitate with the increase in NaOH concentration due to the conversion of the REE phosphates to REE hydroxides. The conversion was also confirmed by XRD analysis of the solid after $NaOH_{(s)}$ treatment. The XRD diffraction peaks are rather large due to the amorphous nature of the precipitate but the XRD pattern is in accordance with the presence of $REE(OH)_{3(s)}$ (Fig. 8). A small amount of $Fe_3O_{4(s)}$ was also observed.

Finally, dissolution tests of the REE hydroxide concentrate were conducted in dilute HCl as recently reported by Hadley and Catovic (2014). Relatively good dissolution rates were obtained at pH 3 and at 70 °C. The dissolution yields were 72%, 81% and 91% for Y, Gd and La, respectively. A small fraction of iron (0.5%) was also dissolved during this step. Moreover, only 18% of the cerium was dissolved. Indeed, Ce(III) is prone to oxidation when in contact with air even in the presence of strongly chelating agents (Deblonde et al., 2013; Zou et al., 2014). Consequently, it is very likely that $CePO_{4(s)}$ is partly converted into $Ce(OH)_{4(s)}$ during the alkaline conversion, which prevents its dissolution in dilute HCl in the next step of the process. However, cerium is less valuable than the other rare earth elements present in the feed solution, so its recovery was not the main goal of this study. Taking into account the phosphate precipitation, the alkaline conversion and the dissolution in HCl, the recovery yields of Y, Gd, La, Ce and Fe were 68%, 77%, 86%, 17% and 1.7% respectively. Efforts will be made to achieve higher yields of recovery for the valuable elements but the results given in this paper demonstrate the possibility of producing REE concentrates from low concentrated industrial solutions which are usually considered as effluents.

5. Conclusion

The recovery of REE from an industrial solution containing 230 mg L^{-1} of REE, 30 mg L^{-1} of Al, 32.3 g L^{-1} of Fe(II) and 75.0 g L^{-1} of SO_4^{2-} was investigated by precipitation with phosphate ions. The REE recovery was higher than 95% when the precipitation is performed at 70 °C, at pH 4 and with a ratio n_{REE}/n_{PO4} of 5 mol/mol. Under these conditions, the precipitation of iron is less than 1%, even under air atmosphere. The results show a substantial decrease of the REE precipitation in the presence of higher concentrations of aluminum. The REE phosphate concentrate can be converted into REE hydroxides by reaction with concentrated $NaOH_{(aq)}$ at boiling point under atmospheric pressure and dissolved in diluted $HCl_{(aq)}$ to produce a purified

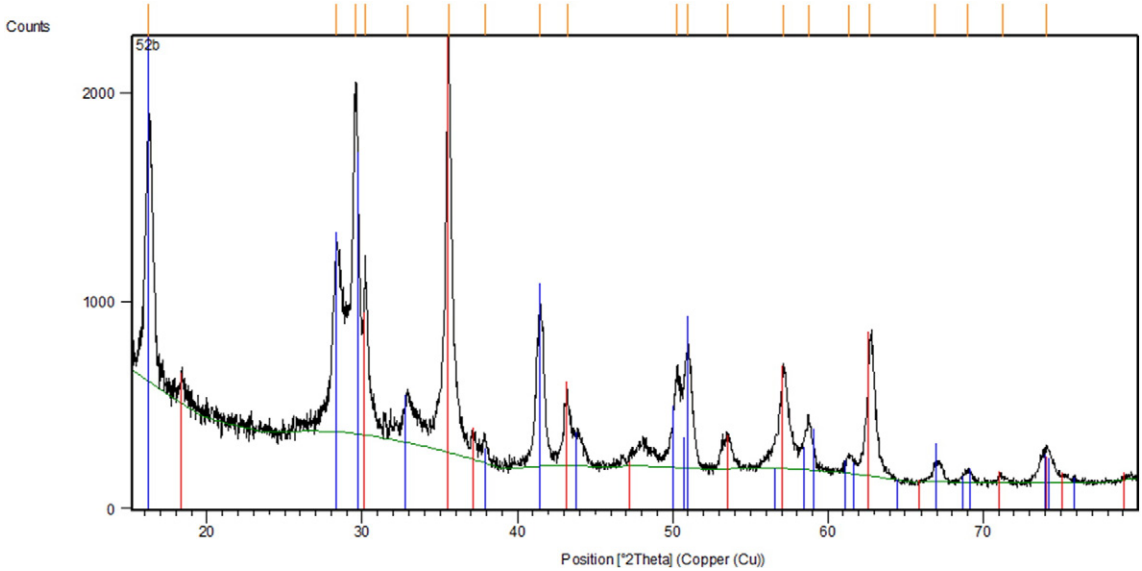

Fig. 8. XRD spectrum of the REE concentrate after alkaline conversion.

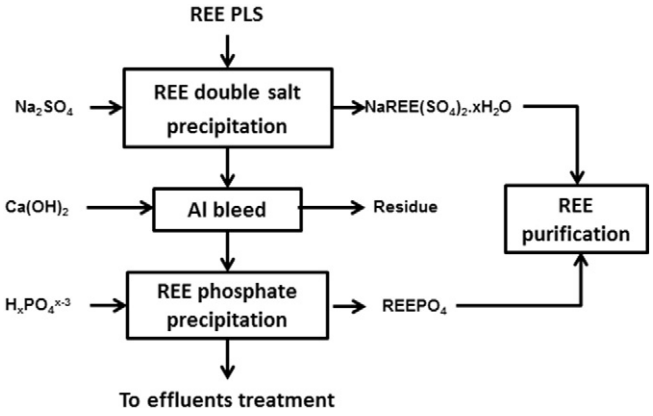

Fig. 9. Proposal flowsheet, elaborated on Al bleed, for the recovery of REE.

REE solution. Finally, the flowsheet given in Fig. 9 is proposed to treat sulfate solutions with high concentration of iron and low REE content. The process developed in this work complements the classical route for REE recovery (i.e. double sulfate salts precipitation) and could help in improving the cost-effectiveness of REE hydrometallurgical processes.

Acknowledgments

The financial support for this work from ERAMET company (France) is gratefully acknowledged. The authors would like to thank Romain Boguais and Cédric Raillard for their help with the experimental part of this study.

Appendix I. Formation constants used to draw the speciation diagrams given in Fig. 4

Reaction	log K	Conditions
$H^+ + HO^- = H_2O$	13.77[a]	I = 0.5 M, T = 25 °C
$PO_4^{3-} + H^+ = HPO_4^{2-}$	11.80[a]	I = 0.5 M, T = 25 °C
$PO_4^{3-} + 2\,H^+ = H_2PO_4^-$	18.34[a]	I = 0.5 M, T = 25 °C
$PO_4^{3-} + 3\,H^+ = H_3PO_4$	20.24[a]	I = 0.5 M, T = 25 °C
$La^{3+} + PO_4^{3-} = LaPO_{4(s)}$	22.43[a]	I = 0.5 M, T = 25 °C
$SO_4^{2-} + H^+ = HSO_4^-$	1.27[a]	I = 0.5 M, T = 25 °C
$La^{3+} + SO_4^{2-} = LaSO_4^+$	1.77[a]	I = 0.5 M, T = 25 °C
$La^{3+} + 2\,SO_4^{2-} = La(SO_4)_2^-$	2.70[a]	I = 0.5 M, T = 25 °C
$La^{3+} + 2\,SO_4^{2-} + Na^+ + H_2O = NaLa(SO_4)_2, H_2O_{(s)}$	6.83[b]	I = 0, T = 20 °C
$La^{3+} + 3\,HO^- = La(OH)_{3,(am)}$	20.30[a]	I = 0, T = 25 °C

[a]: Smith et al. (2004). [b]: Lokshin et al. (2005).

References

Abreu, R.D., Morais, C.A., 2010. Purification of rare earth elements from monazite sulfuric acid leach liquor and the production of high-purity ceric oxide. Miner. Eng. 23, 536–540.
Agin, J., Durupt, N., Greco, A., Hammy, F., Laroche, G., Thiry, J., 2012. Mise en solution et récupération d'au moins un élément Nb, Ta et d'au moins un autre éléments U, terres rares à partir de minerais et concentrés. FR Patent 2970265A1, 13 July 2012.
Alderighi, L., Gans, P., Lenco, A., Peters, D., Sabatini, A., Vacca, A., 1999. Hyperquad simulation and speciation (HySS): a utility program for the investigation of equilibria involving soluble and partially soluble species. Coord. Chem. Rev. 184, 311–318.
Alonso, E., Sherman, A.M., Wallington, T.J., Everson, M.P., Field, F.R., Roth, R., Kirchain, R.E., 2012. Evaluating rare earth element availability: a case with revolutionary demand from clean technologies. Environ. Sci. Technol. 46 (6), 3406–3414.
Anvia, M., Brown, S.A., McOrist, G.D., 2015. The deportment of uranium decay chain radionuclides during processing of an Australian monazite concentrate using caustic conversion route. J. Radioanal. Nucl. Chem. 303 (2), 1393–1398.
Belair, S., Weigel, V., 2014. Maboumine process: a promising process for the developing a polymetallic ore deposit — focus on the downstream part of the process: rare earth recovery. COM 2014 — Conference of Metallurgists Proceedings 978-1-926872-24-7.
Beltrami, D., Cote, G., Mokhtari, H., Courtaud, B., Moyer, B., Chagnes, A., 2014. A review on the recovery of uranium from wet phosphoric acid by solvent extraction processes. Chem. Rev. 114 (24), 12002–12023.
Bian, X., Yin, S.-H., Luo, Y., Wu, W.-Y., 2011. Leaching kinetic of bastnaesite concentrate in HCl solution. Trans. Nonferrous Metals Soc. China 21, 2306–2310.
Binnemans, K., Jones, P.T., Blanpain, B., Van Gerven, T., Yang, Y., Walton, A., Buchert, M., 2013. Recycling of rare earths: a critical review. J. Clean. Prod. 51, 1–22.
Bunus, F., 2000. Uranium and rare earth recovery from phosphate fertilizer industry by solvent extraction. Miner. Process. Extr. Metall. Rev. Int. J. 21 (1–5), 381–478.
Bunus, F., Dumitrescu, R., 1992. Simultaneous extraction of rare earth elements and uranium from phosphoric acid. Hydrometallurgy 28 (3), 331–338.
Bunus, F., Miu, I., Dumitrescu, R., 1994. Simultaneous recovery and separation of uranium and rare earths from phosphoric acid in a one-cycle extraction–stripping process. Hydrometallurgy 35 (3), 375–389.
Chakhmouradian, A.R., Reguir, E.P., Kressall, R.D., Crozier, J., Pisiak, L.K., Sidhu, R., Yang, P., 2015. Carbonatite-hosted niobium deposit at Aley, northern British Columbia (Canada): mineralogy, geochemistry and petrogenesis. Ore Geol. Rev. 64, 642–666.
Deblonde, G.J.-P., Sturzbecher-Hoene, M., Abergel, R.J., 2013. Solution thermodynamic stability of complexes formed with the octadentate hydroxypyridinonate ligand 3,4-LI(1,2-HOPO): a critical feature for efficient chelation of lanthanide(IV) and actinide(IV) ions. Inorg. Chem. 52 (15), 8805–8811.
Donati, L., Courtaud, B., Weigel, V., 2014. Maboumine process: a promising process for the developing a polymetallic ore deposit — focus on the upstream part of the process. Hydromet 2014, Victoria (Canada), June 22–25, 2014.
Esdale, D., Pridmore, D.F., Fritz, F., Muir, P., Williams, P., Coggon, J., 2003. The Olympic Dam copper–uranium–gold–silver–rare earth element deposit, South Australia: a geophysical case history. ASEG Special Publications. 3 pp. 147–168.
Firsching, F.H., Brune, S.N., 1991. Solubility products of the trivalent rare-earth phosphates. J. Chem. Eng. Data 36, 93–95.
Golve, A., Scott, M., Erskine, P.D., Ali, S.H., Ballantyne, G.R., 2014. Rare earths supply chains: current status, constraints and opportunities. Resour. Policy 41, 52–59.
Gupta, C.K., Krishnamurthy, N., 2005. Extractive Metallurgy of Rare Earths. 0-415-33340-7.
Hadley, T., Catovic, E., 2014. Beneficiation and extraction of REE from northern minerals' Browns Range Heavy Rare Earth project. COM 2014 — Conference of Metallurgists Proceedings. ISBN: 978-1-926872-24-7.
Jordens, A., Cheng, Y.P., Walters, K.E., 2013. A review of the beneficiation of rare earth element bearing minerals. Miner. Eng. 41, 97–114.
Kanazawa, Y., Kamitani, M., 2006. Rare earth minerals and resources in the world. J. Alloys Compd. 408–412, 1339–1343.
Kim, E., Osseo-Asare, K., 2012. Aqueous stability of thorium and rare earth metals in monazite hydrometallurgy: Eh–pH diagrams for the systems Th-, Ce-, La-, Nd–(PO_4)–(SO_4)–H_2O at 25 °C. Hydrometallurgy 113–114, 67–78.
Kul, M., Topkayak, Y., Karakaya, I., 2008. Rare earth double sulfates from pre-concentrated bastnasite. Hydrometallurgy 93, 129–135.
Lokshin, E.P., Tareeva, O.A., Ivlev, K.G., Kashulina, T.G., 2005. A study of the solubility of double alkali metal (Na, K) rare earth (La, Ce) sulfates in sulfuric–phosphoric acid solutions at 20 °C. Russ. J. Appl. Chem. 78 (7), 1080–1084.
Lokshin, E.P., Tareeva, O.A., Kashulina, T.G., 2007. A study of the solubility of yttrium, praseodyme, neodyme, and gadolinium sulfate in the presence of sodium and potassium in sulfuric–phosphoric acid solutions at 20 °C. Russ. J. Appl. Chem. 80 (8), 1275–1280.
Mitchell, R.H., 2015. Primary and secondary niobium mineral deposits associated with carbonatites. Ore Geol. Rev. 64, 626–641.
Panda, R., Kumari, A., Jha, M.K., Hait, J., Kumar, V., Kumar, J.R., Lee, J.Y., 2014. Leaching of rare earth metals (REMs) from Korean monazite concentrate. J. Ind. Eng. Chem. 20 (4), 2035–2042.
Pietrelli, L., Bellomo, B., Fontana, D., Montereali, M.R., 2002. Rare earths recovery from NiMH spent batteries. Hydrometallurgy 66, 135–139.
Radhika, S., Kumar, B.N., Kantam, M.L., Reddy, B.R., 2010. Liquid–liquid extraction and separation possibilities of heavy and light rare-earths from phosphoric acid solutions with acidic organophosphorus reagent. Sep. Purif. Technol. 75, 295–302.
Radhika, S., Kumar, B.N., Kantam, M.L., Reddy, B.R., 2011. Solvent extraction and separation of rare-earths from phosphoric acid solutions with TOPS 99. Hydrometallurgy 110, 50–55.
Reddy, B.R., Kumar, B.N., Radhika, S., 2009. Solid–liquid extraction of terbium from phosphoric acid medium using bifunctional phosphinic acid resin, Tulsion CH-96. Solvent Extr. Ion Exch. 27 (5–6), 695–711.
Shannon, R.D., 1976. Revised effective ionic radii and systematic studies of interatomic distances in halides and chalcogenides. Acta Crystallogr. Sect. A: Cryst. Phys., Diffr. Theor. Gen. Crystallogr. 32 (5), 751–767.
Smith, R.M., Martell, A.E., Motekaitis, R.J., 2004. NIST standard reference database 46. NIST Critical Selected Stability Constants of Metal Complexes Database: Version 8.0.
Tan, Q., Li, J., Zeng, X., 2014. Rare earth elements recovery from waste fluorescent lamp: a review. Crit. Rev. Environ. Sci. Technol. http://dx.doi.org/10.1080/10643389.2014.900240.
U.S. Department of Energy, 2011. 2011 Critical Materials Strategy.
Vincec, M., 2014. Procédé de récupération sélective des terres rares d'une solution acide aqueuse de sulfate riche en aluminium. FR Patent 3003270 A1, 9 September 2014.
Wang, L., Long, Z., Huang, X., Yu, Y., Cui, D., Zhang, G., 2010. Recovery of rare earths from wet-process phosphoric acid. Hydrometallurgy 10 (1–2), 41–47.
Xie, F., Zhang, T.A., Dreisinger, D., Doyle, F., 2014. A critical review on solvent extraction of rare earths from aqueous solutions. Miner. Eng. 56, 10–28.
Yang, X., Zhang, J., Fang, X., 2014. Rare earth element recycling from waste nickel–metal hydride batteries. J. Hazard. Mater. 279, 384–388.
Zou, D., Chen, J., Cui, H., Liu, Y., Li, D., 2014. Wet air oxidation and kinetics of cerium(III) of rare earth hydroxides. Ind. Eng. Chem. Res. 53 (35), 13790–13796.